Applied Catalysis B: Environmental 180 (2016) 614–621

Contents lists available at ScienceDirect

Applied Catalysis B: Environmental

journal homepage: www.elsevier.com/locate/apcatb

The electrooxidation of borohydride: A mechanistic study on palladium (Pd/C) applying RRDE, ^{11}B-NMR and FTIR

Christoph Grimmer[a,*], Maximilian Grandi[a], Robert Zacharias[a], Bernd Cermenek[a], Hansjörg Weber[b], Cláudia Morais[c], Têko W. Napporn[c], Stephan Weinberger[a], Alexander Schenk[a], Viktor Hacker[a]

[a] Institute of Chemical Engineering and Environmental Technology, Fuel Cell Systems Group, Graz University of Technology, NAWI Graz, Inffeldgasse 25C, 8010 Graz, Austria
[b] Institute of Organic Chemistry, Graz University of Technology, NAWI Graz, Stremayrgasse 9, 8010 Graz, Austria
[c] IC2MP, Université de Poitiers, 4, Rue Michel Brunet-B27 TSA-51106, 86073 Poitiers Cedex 09, France

ARTICLE INFO

Article history:
Received 1 June 2015
Received in revised form 9 July 2015
Accepted 18 July 2015
Available online 23 July 2015

Keywords:
Electrochemical borohydride oxidation
Palladium catalyst
NMR spectroscopy
FTIR measurements

ABSTRACT

Electrochemical borohydride oxidation reaction, intermediates and reaction products are studied by cyclic voltammetry with rotating disk electrodes, chronoamperometry coupled with ^{11}B NMR spectroscopy and in-situ FTIR measurements. Depending on the electrode potential of a Pd/C catalyst on a rotating disk electrode the number of exchanged electrons varies between four and eight. By employing chronoamperometry the boron species are analyzed during the ongoing reaction with NMR. During all experiments no boron products other than BO_2^- are detected. Incomplete borohydride consumption during the chronoamperometry studies show that the palladium surface is poisoned by an intermediate in the low potential region. In-situ FTIR measurements confirmed that there is no interaction with BH_2-species which are acting as catalyst poison.

1. Introduction

Direct borohydride fuel cells (DBFCs) are of great interest especially for portable applications due to the capability of borohydride anion BH_4^- to deliver up to 8 electrons per molecule at very low potentials of −1.24 V vs. SHE [1]. Sodium borohydride ($NaBH_4$) was first proposed as anodic fuel in 1962, pointing out the benefits of high storage density and long-term stability in alkaline solution [2]. In combination with an oxygen electrode an overall cell voltage of 1.64 V according to the cell Reaction (3) can be obtained [3].

$$BH_4^- + 8OH^- \rightarrow BO_2^- + 6H_2O + 8e^- E^0 = -1.24\,V vs. SHE \quad (1)$$

$$O_2 + 2H_2O + 4e^- \rightarrow 4OH^- E^0 = 0.40V vs. SHE \quad (2)$$

$$BH_4^- + 2O_2 \rightarrow BO_2^- + 2H_2O E^0 = 1.64\,V \quad (3)$$

Despite much effort concerning anode catalyst development the promising advantages of the fuel cannot be fully utilized so far. On the one hand this originates from the fact that the reaction potential is a theoretic thermodynamic concept which cannot be reached in practice. On the other hand the complete oxidation Reaction (1) undergoes complex reaction steps depending on the anode material and the electrode potential [1,4,5].

In general catalysts can be divided into hydrolyzing and non-hydrolyzing materials. Catalysts that show high adsorption tendency of hydrogen such as palladium or platinum belong to the first group [5]. The main side reaction, namely the borohydride hydrolysis Reaction (4), is catalyzed by this kind of materials which lowers the coulombic efficiency and can lead to mechanical stress inside the electrode. Comparing palladium with gold anode catalysts, Pd shows better electrocatalytic activity with an onset potential approx. 200 mV lower but as mentioned above exhibits activity toward the hydrolysis side reaction [4,6].

$$BH_4^- + 2H_2O \rightarrow BO_2^- + 4H_2 \quad (4)$$

There is little literature concerning the reaction mechanism on palladium but several authors assume similar reaction steps to platinum catalysts [7–9]. The hydrolysis is reported to undergo a

* Corresponding author. Fax: +43 316 873 8782.
E-mail addresses: christoph.grimmer@tugraz.at (C. Grimmer), maximilian.grandi@student.tugraz.at (M. Grandi), robert.zacharias@student.tugraz.at (R. Zacharias), bernd.cermenek@tugraz.at (B. Cermenek), hansjoerg.weber@tugraz.at (H. Weber), claudia.gomes.de.morais@univ-poitiers.fr (C. Morais), teko.napporn@univ-poitiers.fr (T.W. Napporn), stephan.weinberger@tugraz.at (S. Weinberger), alexander.schenk@tugraz.at (A. Schenk), viktor.hacker@tugraz.at (V. Hacker).

http://dx.doi.org/10.1016/j.apcatb.2015.07.028
0926-3373/

stepwise reaction on platinum and compete with the electrooxidation. Such a CE mechanism (chemical reaction followed by electrochemical reaction) is reported by Gyenge (Reactions 5 and 6) while the product can further undergo electrooxidation yielding 6 electrons (7), hydrolysis reaction (8) or a combination of both (see Reactions 9 and 10) [1,7,10]:

$$BH_4^- + H_2O \rightarrow BH_3(OH)^- + H_2(C) \quad (5)$$

$$(E)H_2 + 2OH^- \rightarrow 2H_2O + 2e^- \quad (6)$$

$$(E)BH_3(OH)^- + 6OH^- \rightarrow B(OH)_4^- + 3H_2O + 6e^- \quad (7)$$

$$BH_3(OH)^- + 3H_2O \rightarrow B(OH)_4^- + 3H_2(C) \quad (8)$$

$$BH_3OH^- + 3OH^- \rightarrow B(OH)_4^- + 3/2H_2 + 2H_2O + 3e^- \quad (9)$$

$$BH_4^- + xOH^- \rightarrow BO_2^- + (x\text{-}2)H_2O + (4\text{-}1/2x)H_2 + xe^- \quad (10)$$

Yang et al. assume a 4 electron pathway on palladium based on their electrochemical experiments combined with the quantification of gaseous hydrogen (see Reactions 11–13) [9]. The resulting adsorbed hydrogen atoms (reaction 11) can either react electrochemically forming water or chemically forming hydrogen.

$$BH_4^- + 4OH^- \rightarrow BO_2^- + 2H_2O + 4H_{ad} + 4e^- \quad (11)$$

$$H_{ad} + OH^- \rightarrow H_2O + e^- \quad (12)$$

$$H_{ad} + H_{ad} \rightarrow H_2 \quad (13)$$

One of the most widely investigated catalysts is platinum in form of nanodispersed Pt/C as well as in bulk form. Based on electrochemical and kinetic studies Elder and Hickling proposed the following reaction mechanism on platinum with the rate determining step being Reaction (16) [11]:

$$BH_4^- + Pt \leftrightarrow Pt\cdots BH_3 + H^+ + 2e^- \quad (14)$$

$$Pt\cdots BH_3 + OH^- \rightarrow Pt\cdots BH_3OH^- \quad (15)$$

$$Pt\cdots BH_3OH^- \rightarrow Pt\cdots BH_2OH + H^+ + 2e^- \quad (16)$$

$$Pt\cdots BH_2OH + H_2O \rightarrow Pt + BH_2(OH)_2^- + H^+ \quad (17)$$

$$Pt\cdots BH_3OH^- + H_2O \rightarrow Pt + BH_{22}^- + H_2(OH) \quad (18)$$

$$BH_{22}^- + H_2O \rightarrow BH(OH)_3^- + H_2(OH) \quad (19)$$

$$(20)BH_3^- \rightarrow H_2BO_3^- + H_2(OH)$$

According to this reaction sequence there should be at least two reaction intermediates present in the bulk electrolyte, namely $BH_2(OH)_2^-$ and $BH(OH)_3^-$.

Concha et al. investigated the reaction mechanism on bulk platinum employing FTIR techniques [12].

They concluded that the potential range can be divided in four regions; first close to ocp – mainly heterogeneous hydrolysis; second 180–700 mV vs. RHE – formation of BH_3 and BH_2-species; third 700–1100 mV vs. RHE – BO_2 final product is detected; fourth above 1100 mV vs. RHE– BH_2-species decrease. In general they found the rate limiting step to be related to the consumption of BH_2-species contradicting the proposition of Elder and Hickling [11–13]. According to their proposed mechanistic steps similar intermediates namely $BH_2(OH)_2^-$ and BH_2OH should be found in the bulk electrolyte.

Employing Levich and Koutecky-Levich analyses the number of exchanged electrons was investigated with results ranging from 2 to 8 electrons for platinum [4,5,14–17]. Based on these electron counts various mechanisms and intermediates were reported. Furthermore, influences on the mechanisms of electrode morphology and concentration ratios are reported [14,18]. The anodic reactions observed during measurements are even more complicated due to electrooxidation of hydrogen that is evolved by parallel hydrolysis. While reaction intermediates are widely investigated for platinum catalysts utilizing online electrochemical mass spectrometry [19] and FTIR [20,21] there is little comparable data for Pd/C available.

Freitas et al. reported a strong effect of the thickness of the active layer on the electron count. Complete 8 electron oxidation is obtained for 3 μm thick layers while only three electrons are released at layers as thin as 0.38 μm. A smooth platinum surface only yields 2 electrons. Comparable to oxygen reduction reaction it is considered that in thicker layers the intermediates including hydrogen from hydrolysis are trapped and undergo further electrooxidation [14].

As reported by several researchers and can be seen intuitively from the Reaction Eq. (1) the reaction mechanism also strongly depends on the hydroxide concentration or more precisely the concentration ratio $[OH^-]/[BH_4^-]$ [9,18,22]. Liu et al. found a ratio of 5 or higher to be necessary for a complete 8 electron oxidation on gold Au/C and silver Ag/C catalysts and only a 3 electron exchanging mechanism for a ratio of 1 [18].

As can be seen from the short overview above the reaction mechanism is quite complex and still not completely resolved. For further development of anode materials a better understanding of the electrochemical pathway and its influences is necessary. One major aspect that is still not resolved is the aspect of reaction products that are yielded during non-optimal electrooxidation with less than 8 electrons.

To the authors' knowledge there is little information about reaction intermediates in the bulk electrolyte published in literature. One main question remains: is metaborate (BO_2^-) the only product while hydrogen is lost or are there intermediates that can undergo further electrooxidation? Following proposed mechanisms there can be at least two intermediates expected, namely $BH_2(OH)_2^-$ and $BH(OH)_3^-$.

In this paper we present electrochemical experiments on palladium catalysts with subsequent analysis of the reaction products and/or intermediates by ^{11}B nuclear magnetic resonance (NMR) spectroscopy and mechanism studies by in-situ FTIR spectroelectrochemical measurements.

2. Experimental

2.1. Catalyst preparation

Carbon supported palladium nanoparticles (40 wt.% Pd) were synthesized using the instant reduction method [23,24]. For this purpose the proper amount of $PdCl_2$ was dissolved in 20 ml of 0.5 M HCl. In a round bottom flask the appropriate amount of Vulcan XC72R (CABOT) was suspended in a 50/50 mixture of water/2-propanol via ultrasonification for 30 min. To the homogeneous dispersion, the $PdCl_2$ solution was added. The pH was adjusted to 9–10 by adding 1 M NaOH drop wise under vigorous stirring. After heating to 60 °C the mixture was stirred for 5 h before the suspension was saturated with hydrogen. The temperature and the H_2 atmosphere were maintained for another 6 h. The resulting dispersion was filtered and the remaining catalyst was washed several times with ultrapure water and dried overnight at 90 °C.

2.2. Physical characterization

Transition electron microscope experiments are performed using a TF20 TEM (FEI), Schottky cathode, operated at 200 kV equipped with an EDAX Si(Li) detector for EDX acquisition. An aliquot of the Pd/C catalyst was dispersed in an appropriate amount of isopropanol and mounted on standard Cu grids which are covered with perforated carbon film. TEM imaging experiments are conducted at room temperature.

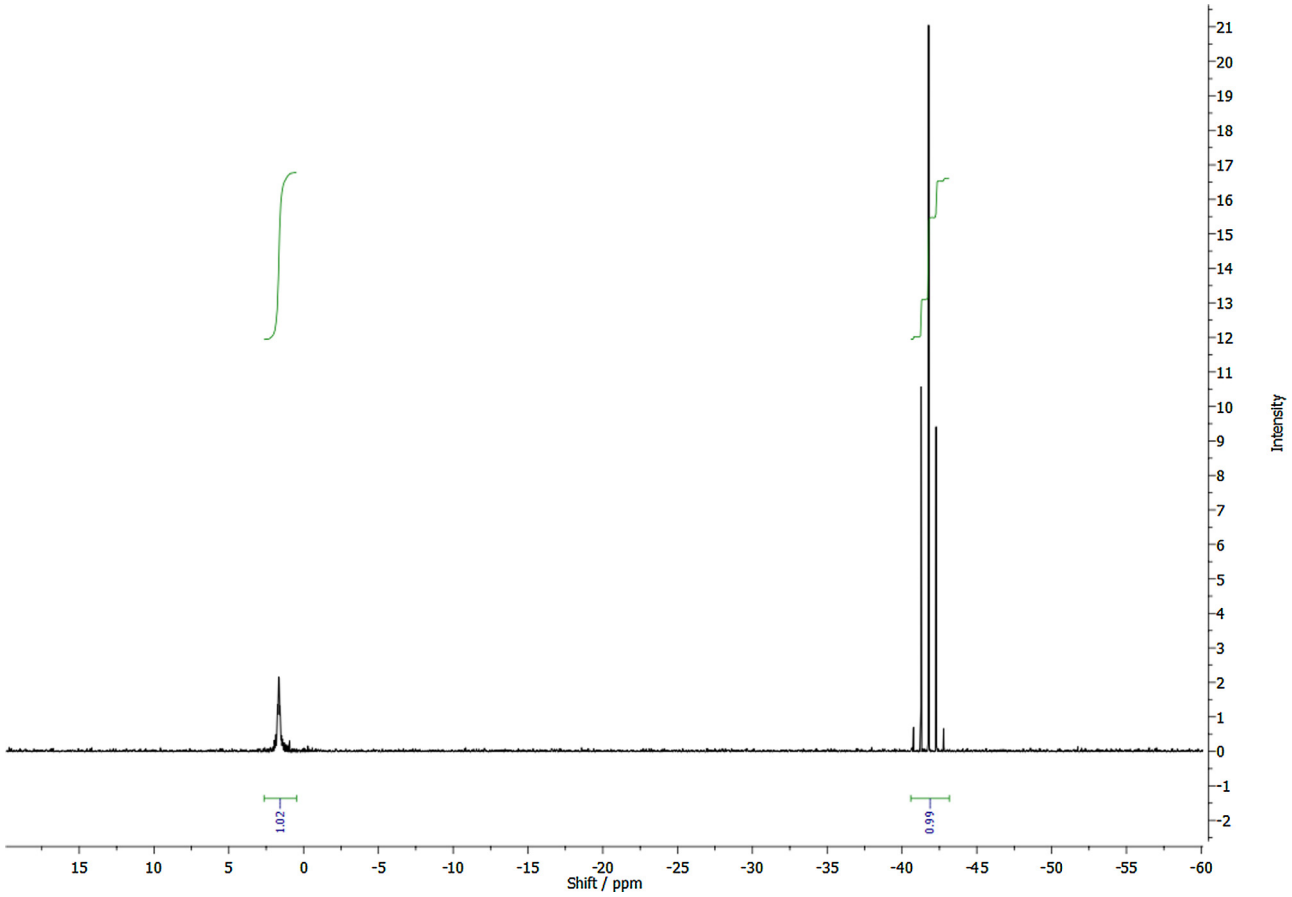

Fig. 1. ^{11}B NMR experiment of an equimolar solution of $NaBH_4$ and $NaBO_2$ in 1 M NaOH with 20%vol. D_2O.

2.3. Electrochemical measurements

The electrochemical measurements were performed with a Gamry Instruments Reference 600 potentiostat (supplied by C3 Analysentechnik, Germany) employing a glassy carbon (GC) rotating disk electrode (RDE) from Pine Industries with a geometric surface area of 0.196 cm^2 in a three electrode configuration. The rotating ring disk electrode (RRDE) consisted of a GC disk (0.247 cm^2) and a Pt ring (collection efficiency 37%, E7R9 series from Pine Industries). The measurement cell temperature was kept at 30 °C. The glassy carbon RDE was polished prior to each measurement to a mirror finish with alumina microsuspension (0.05 μm). A reversible hydrogen electrode (RHE) (gaskatel) and a glassy carbon rod (Metrohm) were used as reference electrode and counter electrode, respectively.

In order to prepare a homogeneous catalyst film the catalyst sample was dispersed in a mixture of 2-propanol/water (7:3), ultrasonificated for 30 min and an aliquot of 10 μl was dispensed on the RDE resulting in a metal loading of 28 μg cm^{-2}. The RDE was rotated at 700 rpm during dry off ensuring a homogeneous and reproducible catalyst layer [25].

The electrolyte consisted of 1 M NaOH (Fixanal, Fluka Analytical) prepared of ultrapure water (18.2 MΩ cm) that was purged with nitrogen for 30 min prior to each measurement.

The catalyst was cycled between 0.05 V to 1.20 V vs. RHE at a scan rate of 50 mV s^{-1} until stable cycles were obtained. Cyclic voltammograms of the Pd/C (40 wt.%) catalysts were recorded between 0.05 V and 1.30 V at a scan rate of 10 mV s^{-1} to determine the electrochemically active surface area (ECSA) by integrating the Pd-O reduction peak considering 405 μC cm^{-2} as conversion factor [26]. RDE and RRDE measurements were carried out after adding $NaBH_4$ with a total concentration of 5 mM at various rotation rates in the potential range of −0.05–1.60 V vs. RHE. The number of exchanged electrons was determined by Levich and Koutecky-Levich analyses [27]. RRDE experiments are conducted at 1600 rpm with fixed ring potentials and cyclic voltammetry on the disk with a scan rate of 10 mV s^{-1}.

At this point we want to stretch out that RDE experiments allow proper insight into catalytic properties of a material. However, the influences of the electrode structure and morphology etc. are not addressed by this technique [28,29].

2.4. Chronoamperometry and NMR measurements

In order to follow the change of the concentration of boron species chronoamperometric measurements were carried out in the same setup at fixed potentials of 0.40 V and 0.80 V vs. RHE with a rotation rate of 1600 rpm. The electrolyte consisted of 1 M NaOH with a starting concentration of $NaBH_4$ of 5 mM. During the measurement samples of 0.40 ml were taken from the electrolyte, 0.10 ml D_2O were added and the NMR measurement was performed instantly.

^{11}B NMR spectra were acquired on a Varian/Agilent 500 MHz Spectrometer tuned to ^{11}B at 160.38 MHz. 64 Scans were accumulated for both 1H-decoupled (Waltz Decoupling 499.87 MHz) and coupled spectra. A 45 degree pulse was used with a relaxation delay of 1 s and 1.022 s acquisition time. Data processing consisted of cutting the first 8 data points, Fourier transform, an automated baseline correction and phase correction by square of the magnitude.

The boron shifts of BH_4^- and BO_2^- and the corresponding integrals of both peaks are verified by measuring an equimolar solution

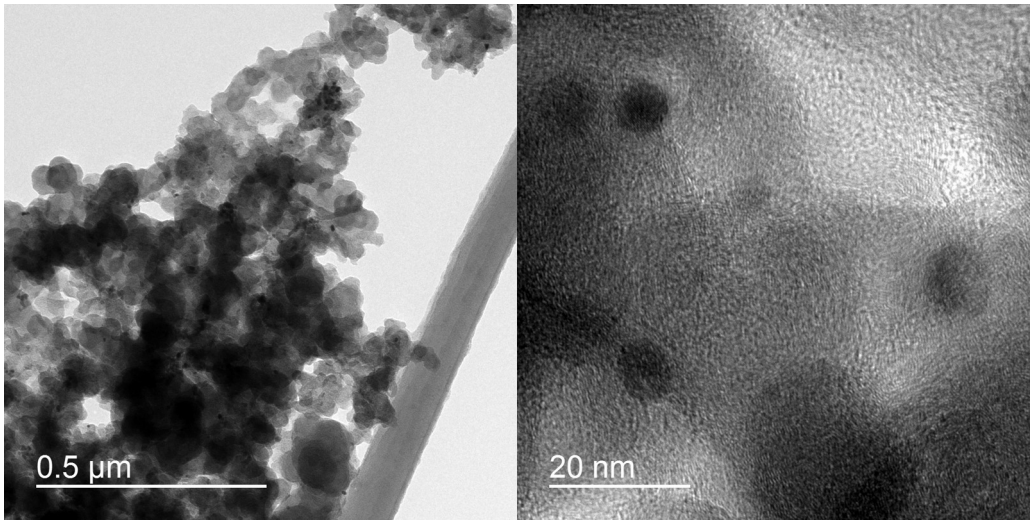

Fig. 2. TEM images of of Pd/C electrocatalyst; left: overview, right: detail view of single particles.

(2.5 mM each, see Fig. 1). We observed matching literature shifts for BO_2^- at 1.65 ppm as singlet and for BH_4^- at −41.8 ppm as quintet [30]. The coulombic efficiency is determined as a ratio of the electric charge of the corresponding experiment to the amount of borohydride considering complete 8 electron oxidation.

2.5. In-situ FTIR measurements

In-situ FTIR measurements were carried out using a Bruker IFS 66 v spectrometer which was modified for beam reflection on the electrode surface at a 65° incidence angle. A 10^{-6} bar vacuum was maintained in order to avoid interferences from atmospheric water and CO_2. The detector was a liquid nitrogen cooled MCT (HgCdTe) type. The spectral resolution was 8 cm^{-1} and the spectra were recorded in the region of 800–4000 cm^{-1}. A three-electrode spectroelectrochemical cell, fitted at the bottom with a mid-infrared (MIR) transparent window (CaF_2) was used. The counter electrode was a glassy carbon electrode, the working electrode was a glassy carbon disk (8 mm diameter) and a RHE was used as reference electrode. To minimize the absorption of the infrared beam by the solution, the working electrode was pressed against the window, resulting in a thin layer of electrolytic solution. A Chronoamperometry/FTIRS study at 0.20, 0.40, 0.60 and 0.80 V vs. RHE, each 40 min, with acquisition of spectra every 5 min, was performed. IR spectra were calculated in terms of changes in the reflectivity (R) relative to a reference single-beam spectrum (R_{ref}) as follows: $(\Delta R/R)_i = (R_i - R_{ref})/R_{ref}$. Positive and negative bands represent the decrease and increase of species, respectively. The deposition of catalyst on the glassy carbon disk, previously polished to a mirror finish, was performed by pipetting 5 µL of a catalyst ink containing 1.68 mg ml^{-1} of Pd. All measurements were performed in 0.1 M NaOH + 50 mM $NaBH_4$ electrolyte.

3. Results and discussion

3.1. TEM images

Transition electron microscopy images show homogeneous dispersed nanoparticles of Pd on carbon substrate material (see Fig. 2). The determined mean particle size is 7.3 ± 1.4 nm which is within the expected scope compared to the electrochemically determined ECSA. EDX analysis confirmed the elemental composition within the inaccuracies especially concerning the quantification of carbon.

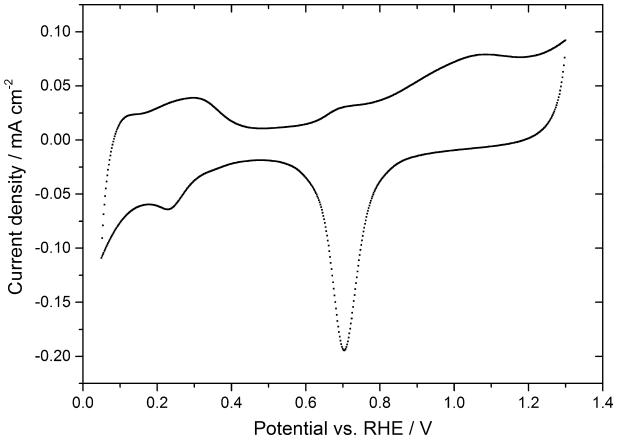

Fig. 3. Cyclic voltammograms of Pd/C in deaerated 1 M NaOH at a scan rate of 10 mV s^{-1}.

3.2. Electrochemical measurements

3.2.1. Cyclic voltammetry

Fig. 3 shows a typical result of cyclic voltammetry experiments of Pd/C in deaerated electrolyte. A well-defined reduction peak of Pd-O is observed with a charge of 422 µC originating from an electrochemical active surface area of 190 cm^2 mg^{-1} Pd. In Fig. 4 a typical cyclic voltammogram with 5 mM $NaBH_4$ in the electrolyte is shown. The anodic sweep exhibits three peaks which can be ascribed to hydrogen oxidation (around 5 mV), direct oxidation of BH_3OH^- which is generated by hydrolysis at 300 mV and direct 8-electron oxidation of borohydride with a broad shoulder starting at 0.80 V [31]. The cathodic sweep shows also three oxidation peaks which can be ascribed to the oxidation of intermediates, which are formed during ongoing hydrolysis and that are adsorbed on the catalyst surface [1].

3.2.2. RDE and RRDE experiments

RDE experiments were conducted at rotations rates up to 2000 rpm. Anodic sweeps of a typical experiment are shown in Fig. 5. As confirmed by Levich analysis (insert) two diffusion limited oxidation regions are observed at around 0.40 V vs. RHE and 0.80 V vs. RHE. Considering 1.67×10^{-5} cm^2 s^{-1} as diffusion coefficient and 0.0114 cm^2 s^{-1} as kinematic viscosity Levich analysis gives a 4-electron oxidation at 0.40 V vs. RHE and an 8-electron oxidation

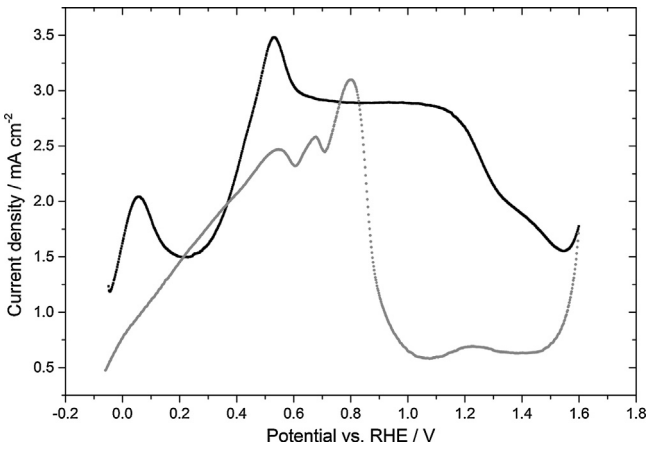

Fig. 4. Cyclic voltammograms of Pd/C in 1 M NaOH containing 5 mM borohydride (black: anodic sweep, gray: cathodic sweep).

at 0.80 V vs. RHE [4,32]. We observed a complete electrooxidation at 0.80 V vs. RHE while at 0.40 V vs. RHE there are two possible pathways: first a complete reaction to BO_2^- releasing 2 hydrogen molecules (see reaction 21) or second a 4-electron electrooxidation resulting in BH_2-species (see Reaction 22). The Levich plot at 0.80 V vs. RHE intercepts at almost zero while the linearization at 0.40 V vs. RHE has a positive value of approx. 3 mA cm^{-2}. The positive intercept indicates also a kinetic limitation at low potentials suggesting adsorbed intermediates.

If the BH_2-species is present either adsorbed on the catalyst surface or in solution is part of the discussion in section 3.3 and 3.4.

$$BH_4^- + 4OH^- \rightarrow BO_2^- + 2H_2O + 2H_2 + 4e^- \quad (21)$$

$$BH_4^- + 4OH^- \rightarrow BH_2(OH)_2^- + 2H_2O + 4e^- \quad (22)$$

For further investigations of the catalytic behavior RRDE experiments were conducted. The reaction mechanism following proposed Reaction (21) would show a hydrogen oxidation at the ring above 0.00 V vs. RHE while Reaction (22) should show oxidation currents only at higher ring potentials. In case of Reaction (21) the evolved hydrogen could be further oxidized in an intelligent three dimensional electrode architecture [14,28]. At thin films on RDEs hydrogen bubbles are swiped away and lost.

The ring current at 0.30 V vs. RHE is below 1.0 mA cm^{-2} and shows the oxidation of hydrogen that evolves during the measurement. At a potential of 0.55 V vs. RHE borohydride is completely oxidized on the metallic platinum ring. The maximum ring current density is about 13 mA cm^{-2} and corresponds the expected value for the given collection efficiency of 37%. The observed current between 0.20 V and 0.80 V vs. RHE and the low current from hydrogen evolution suggest Reaction (22) with adsorbed BH_2-species in the low potential range Fig. 6.

3.3. Chronoamperometry coupled with ^{11}B NMR

Based on the results of RDE and RRDE experiments chronoamperometry measurements were carried out at 0.40 V (4 electron oxidation) and 0.80 V (8 electron oxidation). The experiments were done employing RDEs at a rotation rate of 1600 rpm with subsequent analysis of boron species in the electrolyte by ^{11}B NMR. Based on previous published mechanisms (see discussion above) a reaction intermediate, most likely $BH_2(OH)_2^-$, or the reaction product BO_2^- is expected during oxidation at 0.40 V vs. RHE (see Reactions 21 and 22). A signal for BH_2-species in the NMR spectra would confirm Reaction 22.

Fig. 7 shows the results from chronoamperometry measurements including NMR results. No intermediate could be observed throughout the whole measurement. The current decreases to zero after only three hours although borohydride is still available in the electrolyte (concentration 4.6 mM according to NMR integrals). We conclude that reaction 16 is indeed rate-limiting at 0.40 V vs. RHE but reaction 17 does not occur on Pd at this potential. Most likely Reaction 22 is taking place without desorption of the product $BH_2(OH)_2^-$.

We assume that BH_2^--species adsorb on the surface blocking it for further electrooxidation. By integration of the current an electrical charge of 6.98 C is obtained giving a coulombic efficiency of 97.9% compared with borohydride concentration from NMR (see Table 1).

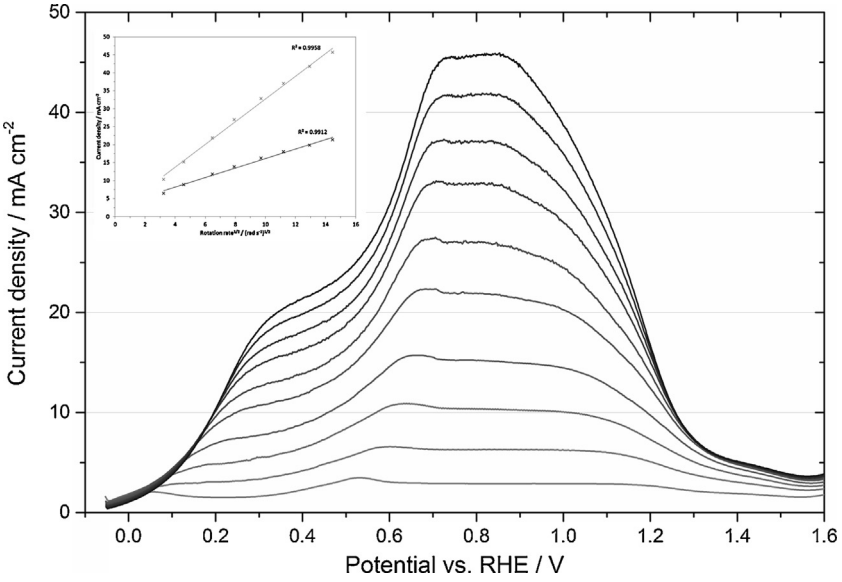

Fig. 5. Anodic sweeps of RDE experiments at 0, 50, 100, 200, 400, 600, 900, 1200, 1600 and 2000 rpm with a scan rate of 10 mV s^{-1} (5 mM $NaBH_4$); insert: according Levich plot at 0.40 V and 0.80 V.

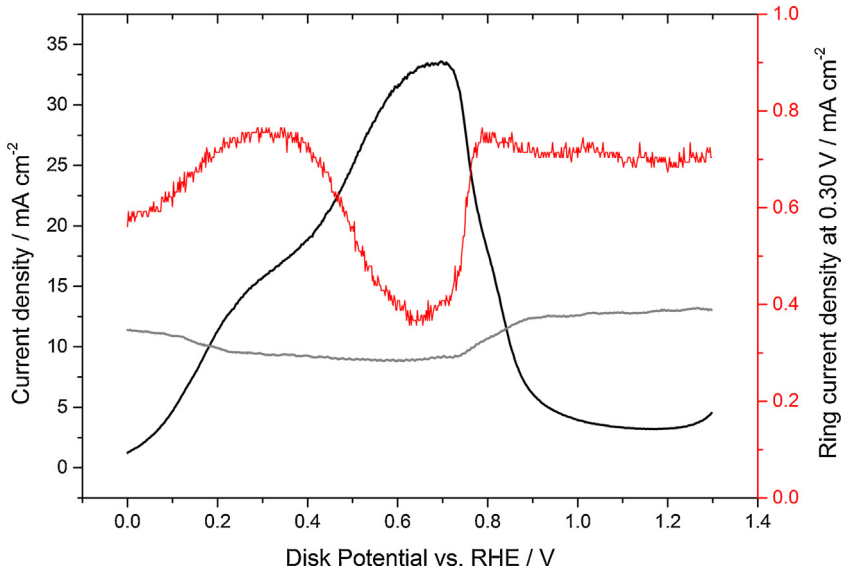

Fig. 6. RRDE experiments at 1600 rpm with a scan rate of 10 mV s^{-1} at the disk and two ring potentials: disk current density (black), ring current density at 0.55 V vs. RHE (gray) and ring current density at 0.30 V vs. RHE (red, secondary axis). (For interpretation of the references to colour in this figure legend, the reader is referred to the web version of this article.)

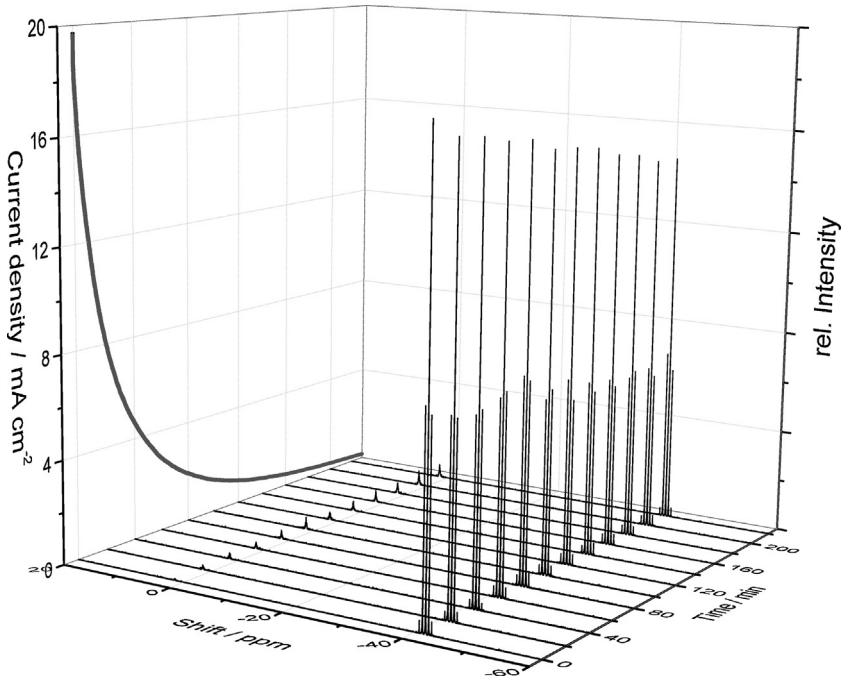

Fig. 7. Chronoamperometry at 0.40 V coupled with subsequent NMR measurements; left *z*-axis: current density of electrochemical measurement; *x*-axis: shift of ^{11}B NMR; *y*-axis: time; right *z*-axis: intensity of NMR signals.

Table 1
Borohydride concentrations before and after chronoamperometric study (by NMR integrals), electric charge obtained by chronoamperometry and coulombic efficiency.

	Start concentration [BH_4^-]	End concentration [BH_4^-]	Charge (Chronoamperometry)	Coulombic efficiency
Low potential	5.0 mM	4.6 mM	6.98 C	97.9%
High potential	5.0 mM	0.0 mM	52.17 C	54.1%

At high potentials the chronoamperometric investigation shows a complete conversion of BH_4^- to BO_2^- (see Fig. 8). Samples for NMR analysis are taken after the current declined 25, 50, 75 and 100%. The decrease of the current with ongoing reaction fits the decreasing concentration of BH_4^- in the electrolyte very well. After the reaction time of 11 h a coulombic efficiency of only 54.1% is observed. As reported for platinum based catalysts the activity toward hydrolysis is increasing with increasing potentials [33]. The adsorbed species seems to poison both reactions, the electrochemical oxidation and the heterogeneous hydrolysis reaction at 0.40 V vs. RHE.

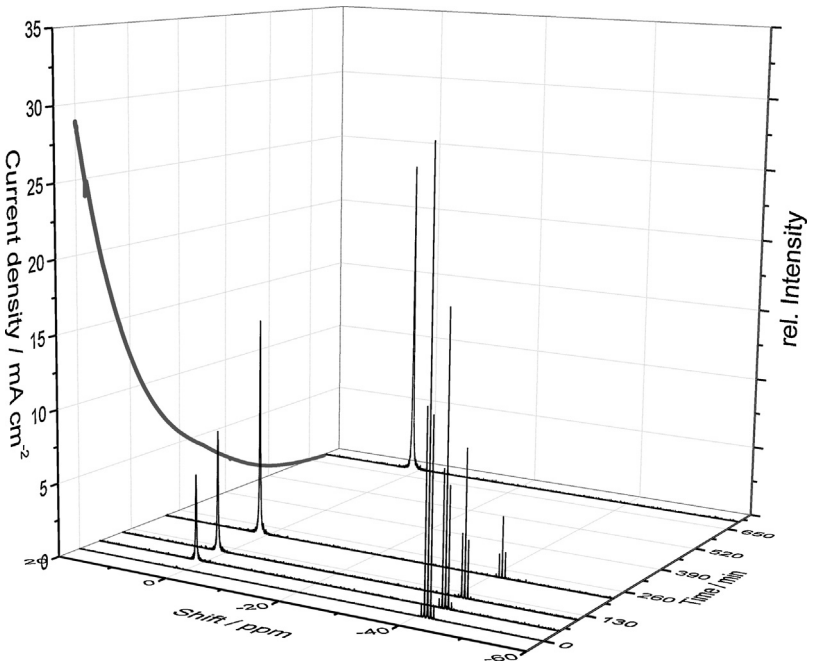

Fig. 8. Chronoamperometry at 0.80 V coupled with subsequent NMR measurements; left *z*-axis: current density of electrochemical measurement; *x*-axis: shift of ^{11}B NMR; *y*-axis: time; right *z*-axis: intensity of NMR signals.

Table 2
IR bands of boron species associated with electrochemical borohydride oxidation [12,20,21].

Band cm^{-1}	Species
973	BH_2
1102	BH_4
1175	BH_3
1650	H_2O deformation
2268	BH_4

3.4. In-situ FTIR measurements

In Table 2 the corresponding IR bands which are used for the interpretation of the results are summarized [12,20,21]. At this point we want to draw attention to the fact that IR bands from electrochemical in-situ IR measurements are influenced by the catalysts' surface [12]. However, the obtained results can be referred to previous published results for platinum based catalysts.

Fig. 9 shows the results of in-situ FTIR measurements from chronoamperometry measurements at various potentials. The absorption bands at the potentials above 0.40 V vs. RHE show similar patterns with the only difference being the intensities. The band at 973 cm^{-1} has been assigned to electrochemical interactions of BH_2 species with the catalysts' surface and is observed at potentials above 0.40 V vs. RHE. A strong adsorption of a species shifts the IR signal and is therefore not observed at these wavenumbers. Since this band cannot be found at 0.20 V vs. RHE these species cannot be further oxidized on palladium at this potential which is also confirmed by RDE measurements. Positive bands at 1102 cm^{-1} and 2268 cm^{-1} correspond to borohydride and indicate its trans-

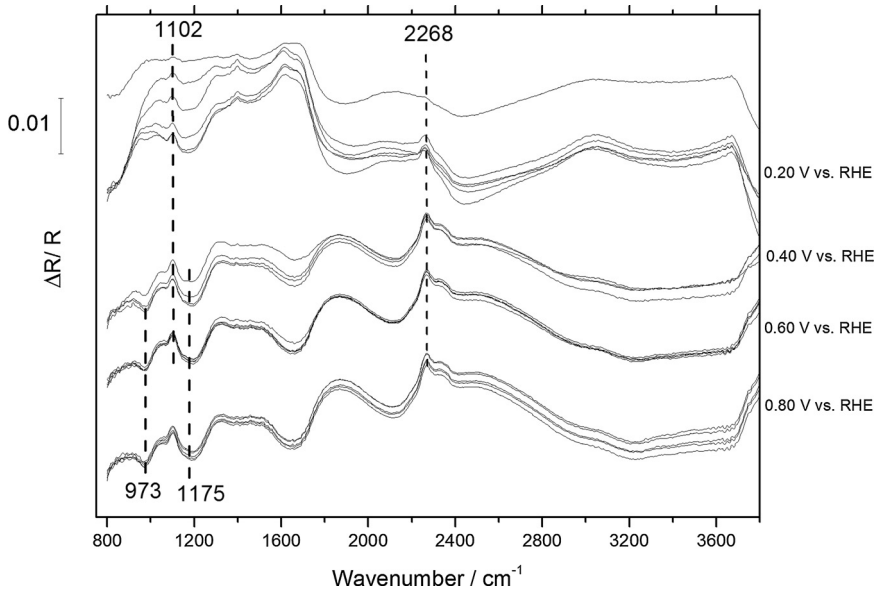

Fig. 9. In-situ FTIR measurement of chronoamperometry at various potentials at Pd/C catalyst, several measurements for each potential taken every 5 min.

formation which starts at very low potential values. At 1175 cm^{-1} a raising negative peak is found at 0.20 V vs. RHE indicating interactions with BH_3-species, which is also present in high potential measurements. In the low potential regime palladium interacts with BH_4^-- and BH_3-species (according Reactions (14) and (16)) resulting in a four electron transfer. In the higher potential regime also BH_2-interactions are detected giving a complete eight electron transfer. The broad negative band at 1650 cm^{-1} is assigned to water deformation indicating the catalytic activity of the hydrolysis reaction especially at elevated potentials, which is also observed by bubble formation during all electrochemical measurements.

Although the potential regimes do not fit perfectly we found a rate-determining step associated with BH_2-species comparable to platinum based catalysts [11]. The shift in potential is attributed to changed electrolyte concentrations which are necessary for the various measurement techniques we employed for our investigations.

4. Conclusion

By the so-called "instant method" palladium nanoparticles with a mean diameter of 7.3 nm were synthesized on carbon support material. RDE measurements and corresponding Levich and Koutecky-Levich analysis show unexpected behavior in low as well as in high potential regimes. In the low potential regime (up to 0.40 V vs. RHE) a maximum of four electrons is obtained while a complete eight electron transfer is obtained at higher potentials. By employing a RRDE we assume the main product $BH_2(OH)_2^-$ to be formed in the low potential regime (reaction 22). Using ^{11}B NMR measurements we traced the borohydride species in bulk solution during chronoamperometry measurements at 0.40 V and 0.80 V vs. RHE. In the low potential region the electrochemical oxidation stops although more than 90% of the origin borohydride is left in the bulk electrolyte. An intermediate which cannot be found in the electrolyte seems to poison the catalytic surface at this potential. By in-situ FTIR measurements we followed the BOR on palladium showing that there is no interaction of BH_2-species with palladium at 0.20 V vs. RHE.

Based on our results we conclude that the intermediate Pd $\cdots$ BH_2OH is blocking the active sites for further electrooxidation in the low potential region (compare Reaction 16). At elevated potentials this intermediate is further oxidized and a complete eight electron transfer is observed. Considering a DBFC application the intermediate could be removed by stopping the borohydride supply inducing an increase of the anode potential.

Acknowledgements

Financial support by the Austrian Federal Ministry of Science, Research and Economics (BMWFW), the Austrian Research Promotion Agency (FFG, project nr. 840476), the IEA research cooperation and our industry partners VTU engineering and proionic GmbH is gratefully acknowledged.

References

[1] E. Gyenge, Electrochim. Acta 49 (2004) 965.
[2] M. Indig, R. Snyder, J. Electrochem. Soc. 109 (1962) 1104.
[3] L.C. Nagle, J.F. Rohan, Int. J. Hydrogen Energy 36 (2011) 10319.
[4] D. Finkelstein, N. Mota, J. Phys. Chem. C 113 (2009) 19700.
[5] A. Tegou, S. Papadimitriou, I. Mintsouli, Catal. Today 170 (2011) 126.
[6] S.S. Muir, X. Yao, Int. J. Hydrogen Energy 36 (2011) 5983.
[7] B.H. Liu, Z.P. Li, S. Suda, Electrochim. Acta 49 (2004) 3097.
[8] I. Merino-Jimenez, M.J. Janik, C. Ponce de Leon, F.C. Walsh, J. Power Sources 269 (2014) 498.
[9] J.Q. Yang, B.H. Liu, S. Wu, J. Power Sources 194 (2009) 824.
[10] J.I. Martins, M.C. Nunes, J. Power Sources 175 (2008) 244.
[11] J.P. Elder, A. Hickling, Trans. Faraday Soc. 58 (1962) 1852.
[12] B.M. Concha, M. Chatenet, E.A. Ticianelli, F.H.B. Lima, J. Phys. Chem. C 115 (2011) 12439.
[13] F.H.B. Lima, A.M. Pasqualeti, M.B. Molina Concha, M. Chatenet, E.A. Ticianelli, Electrochim. Acta 84 (2012) 202.
[14] K.S. Freitas, B.M. Concha, E.A. Ticianelli, M. Chatenet, Catal. Today 170 (2011) 110.
[15] B.M. Concha, M. Chatenet, Electrochim. Acta 54 (2009) 6119.
[16] B.M. Concha, M. Chatenet, Electrochim. Acta 54 (2009) 6130.
[17] B. Šljukić, J. Milikić, D.M.F. Santos, C.A.C. Sequeira, Electrochim. Acta 107 (2013) 577.
[18] B.H. Liu, J.Q. Yang, Z.P. Li, Int. J. Hydrogen Energy 34 (2009) 9436.
[19] M. Chatenet, F.H.B. Lima, E.A. Ticianelli, J. Electrochem. Soc. 157 (2010) B697.
[20] B.M. Concha, M. Chatenet, C. Coutanceau, F. Hahn, Electrochem. Commun. 11 (2009) 223.
[21] B.M. Concha, M. Chatenet, F. Maillard, E.A. Ticianelli, F.H.B. Lima, R.B. de Lima, Phys. Chem. Chem. Phys. 12 (2010) 11507.
[22] M. Mirkin, H. Yang, A. Bard, J. Electrochem. Soc. 139 (1992) 2212.
[23] M.T. Reetz, M. Lopez, Method for in Situ Immobilization of Water-Soluble Nanodispersed Metal Oxide Colloids, WO2003078056, 2003.
[24] R.M. Piasentin, E.V. Spinacé, M.M. Tusi, A.O. Neto, Int. J. Electrochem. Sci. 6 (2011) 2255.
[25] Y. Garsany, I.L. Singer, K.E. Swider-Lyons, J. Electroanal. Chem. 662 (2011) 396.
[26] J. Datta, A. Dutta, S. Mukherjee, J. Phys. Chem. C 115 (2011) 15324.
[27] S. Treimer, A. Tang, D.C. Johnson, Electroanalysis 14 (2002) 165.
[28] C. Ponce de León, S. Kulak, I. Merino-Jiménez, F.C. Walsh, Catal. Today 170 (2011) 148.
[29] I. Merino-Jiménez, C. Ponce de León, A.A. Shah, F.C. Walsh, J. Power Sources 219 (2012) 339.
[30] A.C. Dunbar, J.E. Gozum, G.S. Girolami, J. Organomet. Chem. 695 (2010) 2804.
[31] G. Behmenyar, A.N. Akın, J. Power Sources 249 (2014) 239.
[32] M. Chatenet, M.B. Molina-Concha, N. El-Kissi, G. Parrour, J.-P. Diard, Electrochim. Acta 54 (2009) 4426.
[33] R. Jamard, A. Latour, J. Salomon, P. Capron, A. Martinent-Beaumont, J. Power Sources 176 (2008) 287.